Journal of Marine Science and Technology

Volume 26 | Issue 5 Article 3

THE TREFFTZ TEST FUNCTIONS METHOD FOR SOLVING THE GENERALIZED INVERSE BOUNDARY VALUE PROBLEMS OF LAPLACE EQUATION

Chein-Shan Liu
Center of Excellence for Ocean Engineering, National Taiwan Ocean University, Keelung, Taiwan, R.O.C.

Yung-Wei Chen
Department of Marine Engineering, National Taiwan Ocean University, Keelung, Taiwan, R.O.C.

Jiang-Ren Chang
Department of Systems Engineering and Naval Architecture, National Taiwan Ocean University, Keelung, Taiwan, R.O.C., cjr@mail.ntou.edu.tw

Recommended Citation
Liu, Chein-Shan; Chen, Yung-Wei; and Chang, Jiang-Ren (2018) "THE TREFFTZ TEST FUNCTIONS METHOD FOR SOLVING THE GENERALIZED INVERSE BOUNDARY VALUE PROBLEMS OF LAPLACE EQUATION," *Journal of Marine Science and Technology*: Vol. 26: Iss. 5, Article 3.
DOI: 10.6119/JMST.201810_26(5).0003
Available at: https://jmstt.ntou.edu.tw/journal/vol26/iss5/3

Journal of Marine Science and Technology, Vol. 26, No. 5, pp. 638-647 (2018)
DOI: 10.6119/JMST.201810_26(5).0003

THE TREFFTZ TEST FUNCTIONS METHOD FOR SOLVING THE GENERALIZED INVERSE BOUNDARY VALUE PROBLEMS OF LAPLACE EQUATION

Chein-Shan Liu[1], Yung-Wei Chen[2], and Jiang-Ren Chang[3]

Key words: Laplace equation, generalized boundary value problems, boundary integral equation method, Trefftz test functions.

ABSTRACT

The issue of data completion is important for the elliptic type partial differential equation. In the inverse Cauchy problem, we need to complete the boundary data by over-specifying Dirichlet and Neumann data on a portion of the boundary. In this paper, we numerically solve the generalized inverse boundary value problems of Laplace equation in a rectangle with one boundary function and two boundary functions missing, which are more difficult than the inverse Cauchy problem. By using the technique of a boundary integral equation method together with a specially designed Trefftz test function, we can complete the boundary data by requiring minimal extra data. Then solving the Laplace equation with the given data and recovered data by the multiple-scale Trefftz method, we can find the numerical solution in the interior nodal points.

I. INTRODUCTION

In the past decades there are many numerical methods proposed for solving the inverse Cauchy problems (Yeih et al., 1993; Knowles, 1998; Brühl and Hanke, 2000; Cimetière et al., 2001; Fang and Lu, 2004). Among the many numerical methods, the schemes based on iteration have been developed by Jourhmane and Nachaoui (1999, 2002), Essaouini et al. (2004), Nachaoui (2004), and Jourhmane et al. (2004). Liu (2008a) has applied a modified collocation Trefftz method for the inverse Cauchy problem in a circular domain. In Fu et al. (2007, 2008), a similar method has been named the Fourier regularization method. Liu (2008b) has developed a modified Trefftz method by a simple collocation technique to treat the inverse Cauchy problem of Laplace equation in an arbitrary plane domain. Liu and Kuo (2011), Liu et al. (2011) and Liu and Chang (2012) have proposed the spring-damping regularization techniques to treat the inverse Cauchy problems. Then Liu and Atluri (2013) and Liu (2014) used a better post-conditioning collocation Trefftz method to solve the inverse Cauchy problems.

Previously, the boundary integral equations have been used in Liu and Chang (2016) to recover the space-time dependent heat source, and in Liu (2017) for solving the inverse wave source and backward wave problems. Here we will extend these methods together with the special Trefftz test functions to solve some more difficult generalized inverse boundary value problems. Consider an elliptic type equation, and the bounded domain is denoted by Ω, whose boundary is Γ. For a mixed boundary value problem we specify the Dirichlet boundary data on Γ_1 while the Neumann boundary data on Γ_2, where $\Gamma_1 \cup \Gamma_2 = \Gamma$ and $\Gamma_1 \cap \Gamma_2 = \varnothing$. Otherwise, we encounter the generalized inverse boundary value problems (Liu, 2016; Liu, 2017). Among them, the inverse Cauchy problem is specified as $\Gamma_1 \cup \Gamma_2 \subset \Gamma$ and $\Gamma_1 \cap \Gamma_2 \neq \varnothing$, of which the latter one means that the Cauchy data are over-specified on $\Gamma_1 \cap \Gamma_2$. In the generalized inverse boundary value problem we permit $\Gamma_1 \cap \Gamma_2 = \varnothing$, therefore the concept of "over-specified data" is abandoned, which is named the underspecified inverse Cauchy problem in Liu (2017).

The remaining portion of this paper is arranged as follows. In Section 2 for the Laplace equation in a rectangle, we introduce a boundary integral equation method based on the Green's theorem, which results in a reciprocity gap functional to extract the unknown boundary data from other boundary data. In Section 3, we choose a suitable set of the Trefftz test functions to derive a linear system for the generalized inverse boundary value problem, whose numerical examples are given in Section 4. In Section 5, we derive a boundary integral equation method for the generalized inverse boundary value problem with two boun-

Paper submitted 09/27/17; revised 12/08/17; accepted 08/08/18. Author for correspondence: Jiang-Ren Chang (e-mail: cjr@mail.ntou.edu.tw).
[1] *Center of Excellence for Ocean Engineering, National Taiwan Ocean University, Keelung, Taiwan, R.O.C.*
[2] *Department of Marine Engineering, National Taiwan Ocean University, Keelung, Taiwan, R.O.C.*
[3] *Department of Systems Engineering and Naval Architecture, National Taiwan Ocean University, Keelung, Taiwan, R.O.C.*

dary functions being completed, whose numerical examples are given in Section 6. Finally, the conclusions are drawn in Section 7.

II. BOUNDARY INTEGRAL EQUATION METHOD

1. A Generalized Inverse Boundary Value Problem in a Rectangle

We consider a generalized inverse boundary value problem of the Laplace equation in a rectangle given as follows:

$$\frac{\partial^2 u}{\partial x^2}+\frac{\partial^2 u}{\partial y^2}=0 \tag{1}$$

$$u(x,0)=f(x),\ 0\le x\le a, \tag{2}$$

$$u(x,b)=h(x),\ 0\le x\le a, \tag{3}$$

$$u(0,y)=\ell(y),\ 0\le y\le b, \tag{4}$$

where $f(x)$, $h(x)$ and $\ell(y)$ are given functions. The problem (1)-(4) is an under-specified boundary value problem of the Laplace equation, which has infinite solutions. Our first generalized inverse boundary value problem is how many extra conditions are needed to recover $r(y) = u(a, y)$. If $r(y)$ can be recovered, then the boundary data are completed, and the Laplacian problem is solvable. In Section 5, we will discuss a more difficult problem with only two boundary functions being specified.

2. Green's Second Identity

Before embarking the derivation of Green's second identity for Laplace equation, we introduce the Laplacian operator:

$$\Delta u(x,y)=u_{xx}+u_{yy}. \tag{5}$$

Lemma 1 (Green's Theorem in the plane): Let Ω be a bounded region in the plane (x, y) with a counter-clockwise contour Γ which consists of finitely many smooth curves. Let $F_1(x, y)$ and $F_2(x, y)$ be functions that are differentiable in Ω and continuous on $\bar{\Omega}$. Then

$$\iint_\Omega\left[\frac{\partial F_2}{\partial x}-\frac{\partial F_1}{\partial y}\right]dxdy=\oint_\Gamma\left(F_1dx+F_2dy\right). \tag{6}$$

Letting and inserting

$$F_1=vu_y-uv_y,\ F_2=uv_x-vu_x \tag{7}$$

into Lemma 1, we can prove Green's second identity for the Laplacian operator.

Theorem 1 (Green's second identity): Let Ω be a bounded region in the plane (x, y) with a counter-clockwise contour Γ which consists of finitely many smooth curves. Let $u(x, y)$ and $v(x, y)$ be functions that are twice differentiable in Ω and continuous on $\bar{\Omega}$. Then

$$\iint_\Omega\left[u\Delta v-v\Delta u\right]d\sigma=\oint_\Gamma\left(uv_n-vu_n\right)ds, \tag{8}$$

where $d\sigma= dxdy$ is an area element in the plane and the subscript n denotes the normal derivative with respect to $n = (dy/ds, -dx/ds)$.

Theorem 2 (Global relation for the first problem): For the first generalized inverse boundary value problem in Eqs. (1)-(4), the unknown functions $r(y)$: $= u(a, y)$ and $g(x)$: $= u_y(x, b)$ satisfy the following global relation:

$$\begin{aligned}\oint_\Gamma\left(uv_n-vu_n\right)ds=&-\int_0^a u(x,0)v_y(x,0)dx-\int_0^b r(y)v_x(a,y)dy\\&-\int_0^a\left[u(x,b)v_y(x,b)-v(x,b)g(x)\right]dx\\&-\int_0^a u(0,y)v_x(0,y)dy=0\end{aligned} \tag{9}$$

for any function v with $\Delta v = 0$ and $v(0, y) = v(a, y) = v(x, 0) = 0$. Here the data of $u(x, 0) = f(x)$, $u(x, b) = h(x)$ and $u(0, y) = \ell(y)$ are prescribed.

Proof:

Inserting $\Delta u = 0$ and $\Delta v = 0$ into Eq. (8), integrating along the contour $\Gamma=\Gamma_1\cup\Gamma_2\cup\Gamma_3\cup\Gamma_4$ = $\{0\le x\le a,\ y=0\}\cup\{x=a,\ a\le y\le b\}\cup\{0\le x\le a,\ y=b\}\cup\{x=0,\ 0\le y\le b\}$, and inserting the corresponding conditions in Eqs. (2)-(4), we can prove this theorem.

III. THE NUMERICAL ALGORITHM OF BOUNDARY INTEGRAL EQUATION METHOD

In Theorem 2, we can choose a simple function $v(x, y)$ such that Eq. (9) can be easily used to solve $r(y)$ and $g(x)$. For this purpose, we can take

$$v_k(x,y)=\sin\frac{k\pi x}{a}\left[\exp\left(\frac{k\pi(y-b)}{a}\right)-\exp\left(\frac{-k\pi(y+b)}{a}\right)\right], \tag{10}$$

which is a stable solution of the Laplace equation with $k \in N$ being a positive integer. We may call $v_k(x, y)$ the Trefftz test functions, because they satisfy the Laplace equation automatically. Due to this reason, we may call the present technique a Trefftz test function method. $v_k(x, y)$ is the most simple and useful Trefftz test function for the first problem, which renders three functions $u_x(0, y)$, $u_x(a, y)$ and $u_y(x, 0)$ disappearing from Eq. (9), due to $v_k(0, y) = v_k(a, y) = v_k(x, 0) = 0$. Otherwise, Eq. (9) will be too complicated to use in the solution of the first problem. There exists no Trefftz test function, which is zero on four boundaries; otherwise $v_k(x, y) = 0$ according to the maximum principle of Laplace equation.

Since $v_k(x, b) \neq 0$, in Eq. (9) there still has one term $v_k(x, b)g(x)$ in the integral. If $g(x)$ is prescribed as an extra condition, we have over-specified data on $y = b$. Hence, we encounter an inverse Cauchy problem to recover $r(y)$ on $x = a$ by using the over-specified data on $y = b$. However, we are interested to solve a more difficult problem for the generalized inverse boundary value problem with $g(x)$ being an unknown function. Therefore, we have two unknown boundary functions $r(y)$ and $g(x)$ to be recovered, which are supposed to be

$$r(y) = \sum_{j=1}^{m_1} a_j s_j^1 y^{j-1}, \quad (11)$$

$$g(x) = \sum_{k=1}^{m_2} b_k s_k^2 x^{k-1}. \quad (12)$$

Inserting them and Eq. (10) into Eq. (9) and letting $k = 1, \ldots, m_0$ we can derive a linear system:

$$\mathbf{Ac} = \mathbf{e}, \quad (13)$$

to determine the expansion coefficients a_j, b_k whose number is $n = m_1 + m_2$. The multiple-scales (s_j^1, s_k^2) are determined by the equilibrated method (Liu, 2012, 2013).

Also we have some compatibility conditions and impose some discrete measured data to help the identification of the unknown functions $r(y)$ and $g(x)$:

$$r(0) = u(a, 0), \; r(b) = u(a, b), \quad (14)$$

Case (a) $g(x_i) = g_i, \; x_i = (i-1)a/(m_3 - 1), \; i = 1, \ldots, m_3,$

Case (b) $r(y_j) = r_j, \; y_j = jb/(m_3 + 1), \; j = 1, \ldots, m_3, \quad (15)$

where m_3 is a small number. For the case (a), because some Neumann data are over-specified on the top side $y = b$ of the rectangle where the Dirichlet data are already specified in Eq. (3), it is one of the Cauchy problem but with fewer over-specified data.

The compatibility conditions in Eq. (14) provide two linear algebraic equations as follows:

$$a_1 s_1^1 = u(a, 0), \; \sum_{i=1}^{m_1} a_i s_i^1 b^{i-1} = u(a, b).$$

The dimension of $\mathbf{A}$ is $n_q \times n$ where $n_q = m_0 + 2 + m_3$ is usually greater than n, such that Eq. (13) is an over-determined system. Let $\mathbf{a}_i$ denote the ith column of the coefficient matrix $\mathbf{A}$. Then s_j^1 and s_j^2 are determined as follow:

$$s_i^1 = \frac{\|\mathbf{a}_1\|}{\|\mathbf{a}_i\|}, \; i = 1, \ldots m_1, \quad (16)$$

$$s_j^2 = \frac{\|\mathbf{a}_1\|}{\|\mathbf{a}_{m_1+j}\|}, \; j = 1, \ldots m_2. \quad (17)$$

Therefore, $s_1^1 = 1$ and the norms of all columns of the coefficient matrix $\mathbf{A}$ are equal to $\|\mathbf{a}_1\|$, where $\|\mathbf{a}_1\|$ is the Euclidean norm of the vector $\mathbf{a}_1$.

Instead of Eq. (13), we can solve a normal linear system:

$$\mathbf{Dc} = \mathbf{b}_1, \quad (18)$$

where

$$\mathbf{b}_1 := \mathbf{A}^{\mathrm{T}}\mathbf{e}, \; \mathbf{D} := \mathbf{A}^{\mathrm{T}}\mathbf{A} > \mathbf{0}. \quad (19)$$

The algorithm of conjugate gradient method (CGM) for solving Eq. (18) is summarized as follows.

(1) Give an initial $\mathbf{c}_0$ and then compute $\mathbf{r}_0 = \mathbf{Dc}_0 - \mathbf{b}_1$ and set $\mathbf{p}_0 = \mathbf{r}_0$.
(2) For $k = 0, 1, 2, \ldots$, we repeat the following iterations:

$$\begin{aligned}
\eta_k &= \frac{\|\mathbf{r}_k\|^2}{\mathbf{p}_k^{\mathrm{T}}\mathbf{Dp}_k}, \\
\mathbf{c}_{k+1} &= \mathbf{c}_k - \eta_k \mathbf{p}_k, \\
\mathbf{r}_{k+1} &= \mathbf{Dc}_{k+1} - \mathbf{b}_1, \\
\alpha_{k+1} &= \frac{\|\mathbf{r}_{k+1}\|^2}{\|\mathbf{r}_k\|^2}, \\
\mathbf{p}_{k+1} &= \alpha_{k+1}\mathbf{p}_k + \mathbf{r}_{k+1}.
\end{aligned} \quad (20)$$

If $\mathbf{c}_{k+1}$ converges according to a given stopping criterion $\|\mathbf{r}_{k+1}\| < \varepsilon$, then stop; otherwise, go to step (2).

In view of the numerical algorithm, the key point is the introduction of the Trefftz test functions in Eq. (10), which is limited to the rectangular domain. For the purpose to render $v_k(0, y) = v_k(a, y) = v_k(x, 0) = 0$, Eq. (10) is the unique choice, where we place $k\pi(y - b)$ instead of $k\pi y$ for the stability. Then, - $k\pi(y + b)$ must appear for satisfying $v_k(x, 0) = 0$. In an irregular domain, there exists no such a closed-form Trefftz test function. We also consider the Neumann boundary condition with $u_y(x, b) = g(x)$ to be recovered. If other boundary conditions are specified, the problem is more complicated, of which we must develop another type Trefftz test function. One limitation for the use of Eq. (10) is that b cannot be a large number;

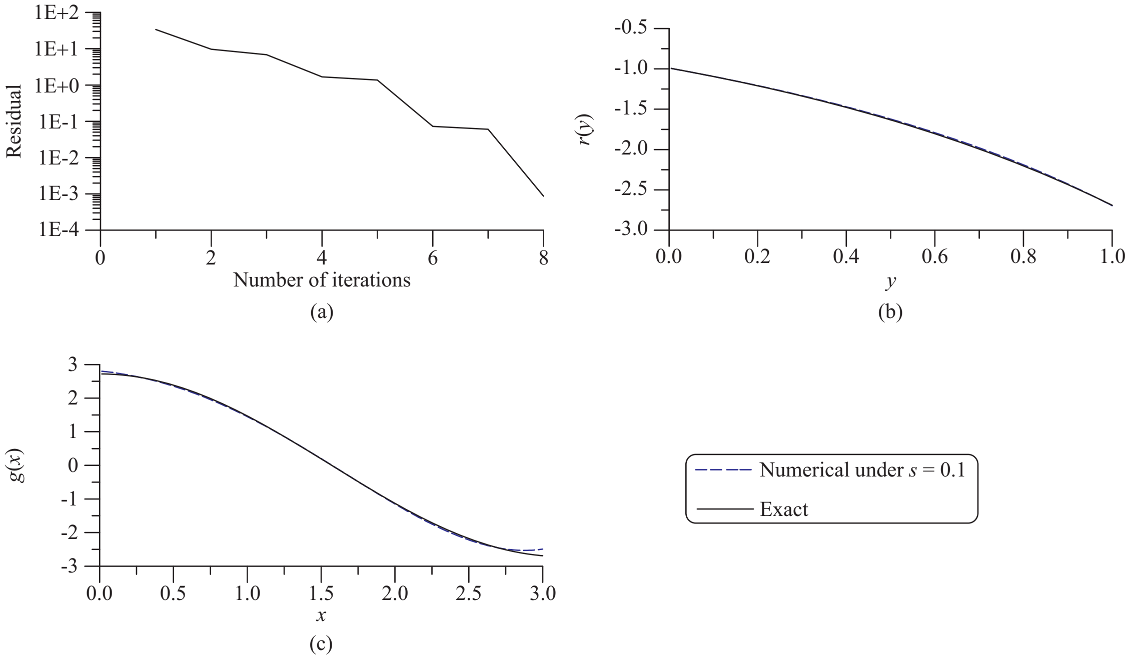

Fig. 1. For case (a) of the first generalized inverse boundary value problem, (a) convergence rate, and comparing numerical and exact solutions of (b) $r(y)$, and (c) $g(x)$ for example 1.

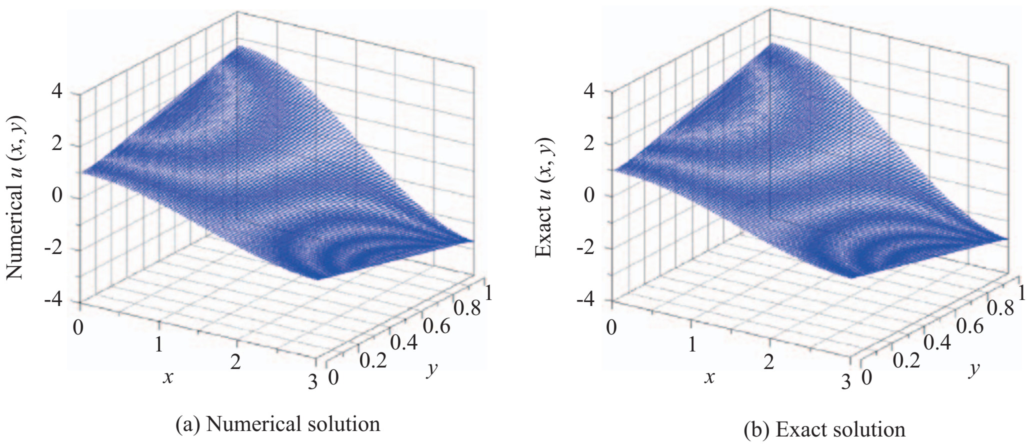

Fig. 2. When unknown boundary data are recovered we apply the multiple-scale Trefftz method to recover the data at interior nodes, (a) numerical solution, and (b) exact solution of example 1.

otherwise, the test functions $v_k(x, y)$ are very weak due to both exponential functions tending to zero.

IV. NUMERICAL EXAMPLES FOR THE FIRST PROBLEM

In this section, we first apply the boundary integral equation method (BIEM) to solve the first generalized inverse boundary value problem for the recovery of $r(y) = u(a, y)$ and $g(x) = u_y(x, b)$. When the boundary data $r(y) = u(a, y)$ are recovered, we can apply the multiple-scale Trefftz method (Liu and Atluri, 2013) to recover the data at interior nodes by

$$u(r, \theta) = a_0 + \sum_{j=1}^{m} a_j s_j^1 r^j \cos j\theta + b_j s_j^2 r^j \sin j\theta, \qquad (21)$$

where the $n = 2m+1$ coefficients $\{a_0, a_j, b_j, j = 1, \ldots, m\}$ can be solved from a linear system by using the CGM given in Section 3, upon imposing the boundary conditions (2)-(4) and $u(a, y) = r(y)$, where $r(y)$ is computed from Eq. (11), at n_c collocation points on the rectangle. In general, $n_c \geq n$. In the CGM we solve the normal linear system, where the convergence criterion is given by ε_1.

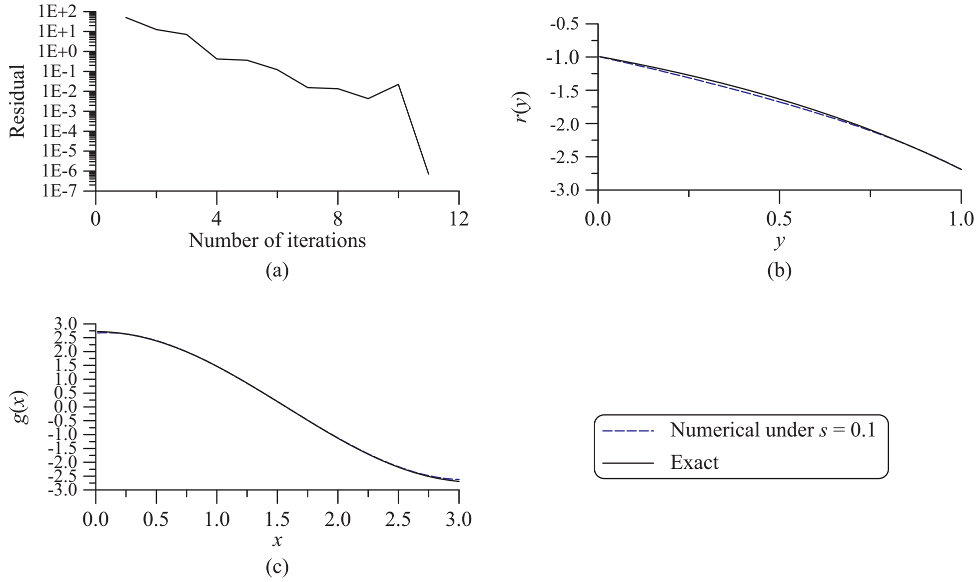

Fig. 3. For case (b) of the first generalized inverse boundary value problem, (a) convergence rate, and comparing numerical and exact solutions of (b) $r(y)$, and (c) $g(x)$ for example 2.

1. Example 1

In order to explore the applicability of the new method, we consider

$$u(x, y) = e^{y} \cos x . \tag{22}$$

We take $a = 3$, $b = 1$, $m_1 = 6$, $m_2 = 5$, $m_3 = 10$ (for case (a)), and $m_0 = 4$, where the measured Neumann data at the top side are added by a relative noise with an intensity s. Although under a large noise $s = 0.1$, the BIEM is convergence with 8 steps as shown in Fig. 1(a), where the convergence criterion is given by $\varepsilon = 10^{-3}$. In Fig. 1(b), we compare the numerical recovery of $r(y)$ with the exact one, whose maximum error is 1.45×10^{-2}. On the other hand, in Fig. 1(c) we compare the numerical recovery of $g(x)$ with the exact one, whose maximum error is 1.99×10^{-1}.

In Fig. 2 we compare the numerically recovered solution at $n_1 \times n_2 = 300 \times 100$ interior nodes to the exact one, where we use $m = 10$ and $\varepsilon_1 = 10^{-5}$. It can be seen that these two solutions are very close with the maximum error being 1.45×10^{-2}.

2. Example 2

Then we consider case (b) with the same solution as that in example 1, where we take $a = 3$, $b = 1$, $m_1 = 6$, $m_2 = 4$, $m_3 = 1$ (for case (b)), and $m_0 = 7$. Although under a large noise $s = 0.1$, the BIEM is convergence with 11 steps as shown in Fig. 3(a), where the convergence criterion is given by $\varepsilon = 10^{-5}$. In Fig. 3(b), we compare the numerical recovery of $r(y)$ with the exact one, whose maximum error is 4.68×10^{-2}, while the numerical recovery of $g(x)$ with the exact one is shown in Fig. 3(c), whose maximum error is 7.03×10^{-2}. It is interesting that we can recover both $r(y)$ and $g(x)$ by merely measuring one extra datum at the middle point on $x = a$.

3. Example 3

We consider

$$u(x, y) = x^3 - 3xy^2 + y^3 - 3x^2 y , \tag{23}$$

and take $a = 1$, $b = 1$, $m_1 = 4$, $m_2 = 5$, $m_3 = 3$ (for case (a)), and $m_0 = 4$. Although under a large noise $s = 0.1$, the BIEM is convergence with 9 steps as shown in Fig. 4(a), where the convergence criterion is given by $\varepsilon = 10^{-3}$. In Fig. 4(b), we compare the numerical recovery of $r(y)$ with the exact one, which are close with the maximum error being 6.7×10^{-2}. In Fig. 4(c), we compare the numerical recovery of $g(x)$ with the exact one, whose maximum error is 2.1×10^{-2}.

When we take $a = 2$ and $b = 2$ for considering a larger domain, and other parameters are unchanged, the BIEM is convergent with 9 steps as shown in Fig. 5(a). In Fig. 5(b) we compare the numerical recovery of $r(y)$ with the exact one, which are close with the maximum error being 4.94×10^{-2}. In Fig. 5(c) we compare the numerical recovery of $g(x)$ with the exact one, whose maximum error is 8.4×10^{-1}.

4. Example 4

Then we consider case (b) for

$$u(x, y) = e^{y} \cos x + x^3 - 3xy^2 + y^3 - 3x^2 y , \tag{24}$$

where $m_1 = 6$, $m_2 = 4$, $m_3 = 1$ (for case (b)), and $m_0 = 7$. Although under a large noise $s = 0.2$, the BIEM is convergence with 7

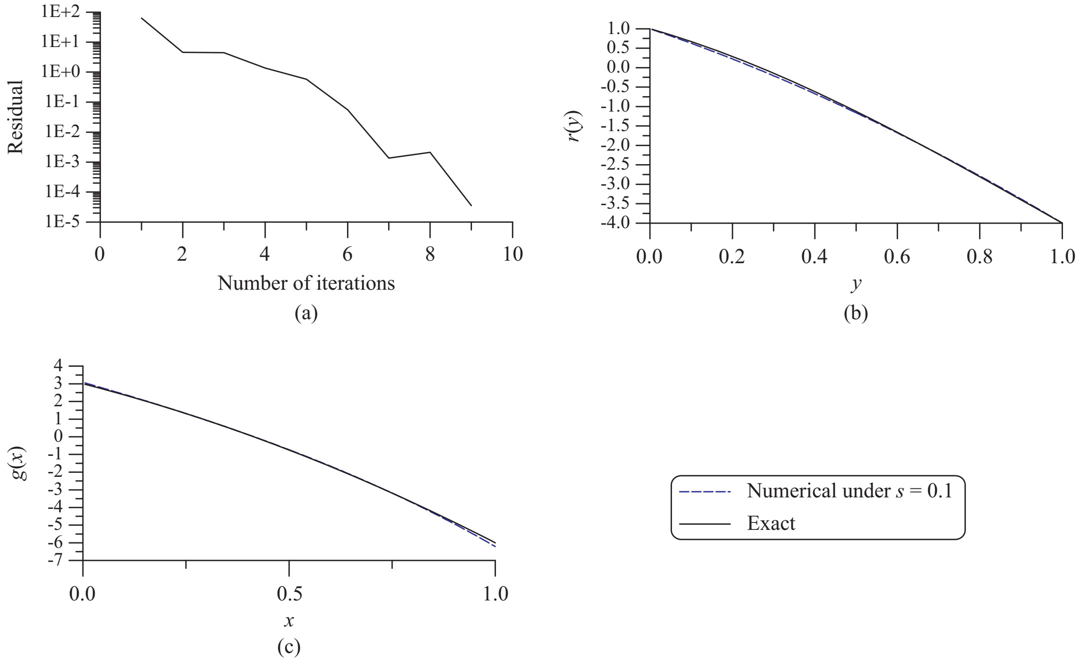

Fig. 4. For case (a) of the first generalized inverse boundary value problem, (a) convergence rate, and comparing numerical and exact solutions of (b) $r(y)$, and (c) $g(x)$ for example 3.

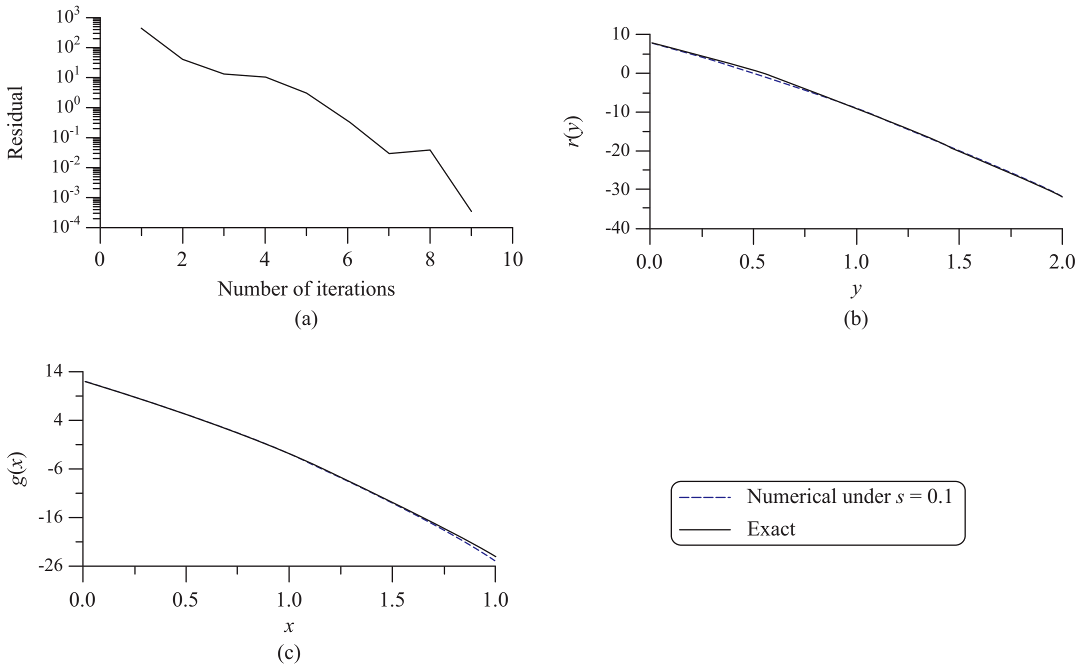

Fig. 5. For a larger domain with case (a) of the first generalized inverse boundary value problem, (a) convergence rate, and comparing numerical and exact solutions of (b) $r(y)$, and (c) $g(x)$ for example 3.

steps as shown in Fig. 6(a), where the convergence criterion is given by $\varepsilon = 10^{-3}$. In Fig. 6(b), we compare the numerical recovery of $r(y)$ with the exact one, whose maximum error is 3.01×10^{-2}, while the numerical recovery of $g(x)$ with the exact one is shown in Fig. 6(c), whose maximum error is 9.05×10^{-2}.

V. THE RECOVERY OF TWO UNKNOWN BOUNDARY DATA

We further consider a more difficult generalized inverse boundary value problem with two boundary data missing:

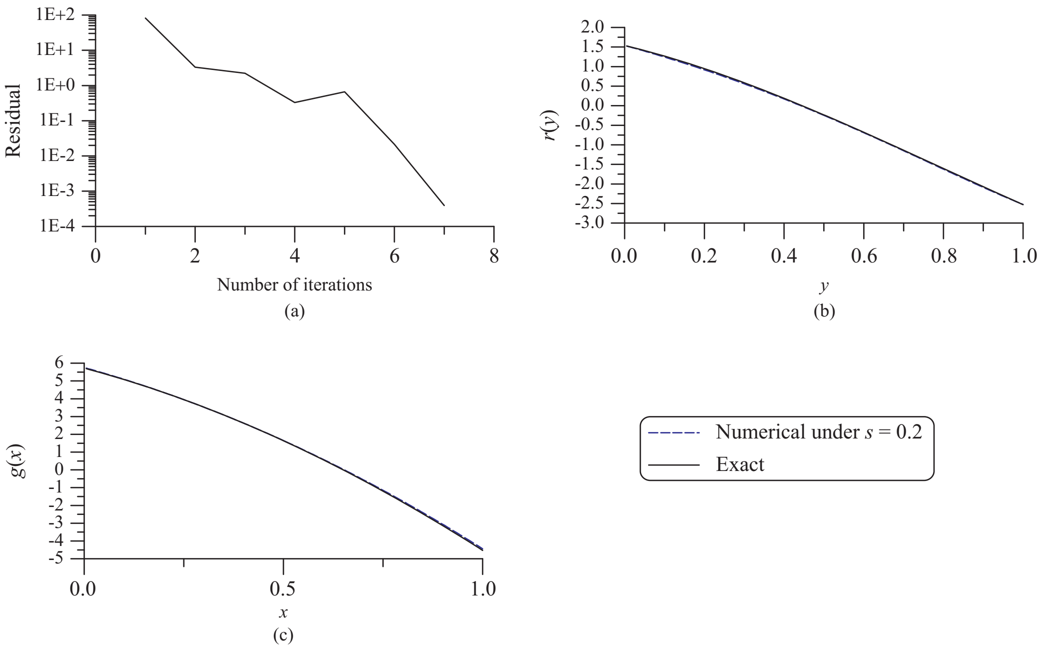

Fig. 6. For case (b) of the first generalized inverse boundary value problem, (a) convergence rate, and comparing numerical and exact solutions of (b) $r(y)$, and (c) $g(x)$ for example 4.

$$\frac{\partial^2 u}{\partial x^2}+\frac{\partial^2 u}{\partial y^2}=0\ ,\ 0<x<a\ ,\ 0<y<b \tag{25}$$

$$u(x, 0)=f(x)\ ,\ 0\le x\le a\ , \tag{26}$$

$$u(0, y)=\ell(y)\ ,\ 0\le y\le b\ , \tag{27}$$

where $f(x)$ and $\ell(y)$ are given functions. Our second generalized inverse boundary value problem is that can we recover $r(y) = u(a, y)$ and $h(x) = u(x, b)$, and how many extra conditions are needed to recover $r(y) = u(a, y)$ and $h(x) = u(x, b)$. If $r(y)$ and $h(x)$ can be recovered, then the boundary data are complete, and the Laplacian problem is solvable. Replacing $u(x, b)$ by $h(x)$ in Theorem 2, it follows that

Theorem 3 (Global relation for the second problem): For the second generalized inverse boundary value problem in Eqs. (25)-(27), the unknown functions $r(y){:}= u(a, y)$ and $h(x){:}= u(x, b)$ and $g(x){:}= u_y(x, b)$ satisfy the following global relation:

$$\begin{aligned}&\int_0^b r(y)v_x(a, y)dy+\int_0^a h(x)v_y(x, b)dx-\int_0^a g(x)v(x, b)dx\\&=\int_0^a u(x, 0)v_y(x, 0)dx+\int_0^b u(0, y)v_x(0, y)dy\end{aligned} \tag{28}$$

for any function v with $\Delta v = 0$ and $v(0, y) = v(a, y) = v(x, 0) = 0$. Here the data of $u(x, 0) = f(x)$ and $u(0, y) = \ell(y)$ are prescribed.

VI. THE NUMERICAL ALGORITHM FOR THE SECOND PROBLEM AND EXAMPLES

To solve the second problem we also take $v_k(x, y)$ as that in Eq. (10). Let

$$r(y)=\sum_{i=1}^{m_1} a_i\, s_i^1 y^{i-1}\ , \tag{29}$$

$$h(x)=\sum_{j=1}^{m_2} b_j\, s_j^2 x^{j-1}\ , \tag{30}$$

$$g(x)=\sum_{k=1}^{m_2} c_k s_k^3 x^{k-1}\ . \tag{31}$$

Inserting them and Eq. (10) into Eq. (28) and letting $k = 1, \ldots, m_0$, and also considering some compatibility conditions and some discrete measured data:

$$r(0)=u(a, 0)\ ,\ h(0)=u(0, b)\ ,\ r(b)=h(a)\ , \tag{32}$$

$$\begin{aligned}&r(y_j)=r_j\ ,\ y_j=jb/(m_4+1)\ ,\ j=1,\ldots, m_4\ ,\\&h(x_i)=h_i\ ,\ x_i=ia/(m_5+1)\ ,\ i=1,\ldots, m_5\ ,\end{aligned} \tag{33}$$

where m_4 and m_5 are small number, we can derive a linear system (13) to determine the expansion coefficients a_i, b_j, c_k whose number is $n = m_1 + m_2 + m_3$.

1. Example 5

We consider the same solution in Eq. (24), where a =1, b = 1, m_1 = 6, m_2 = 6, m_3 = 3, m_4 = m_5 = 6, and m_0 = 5. Although under

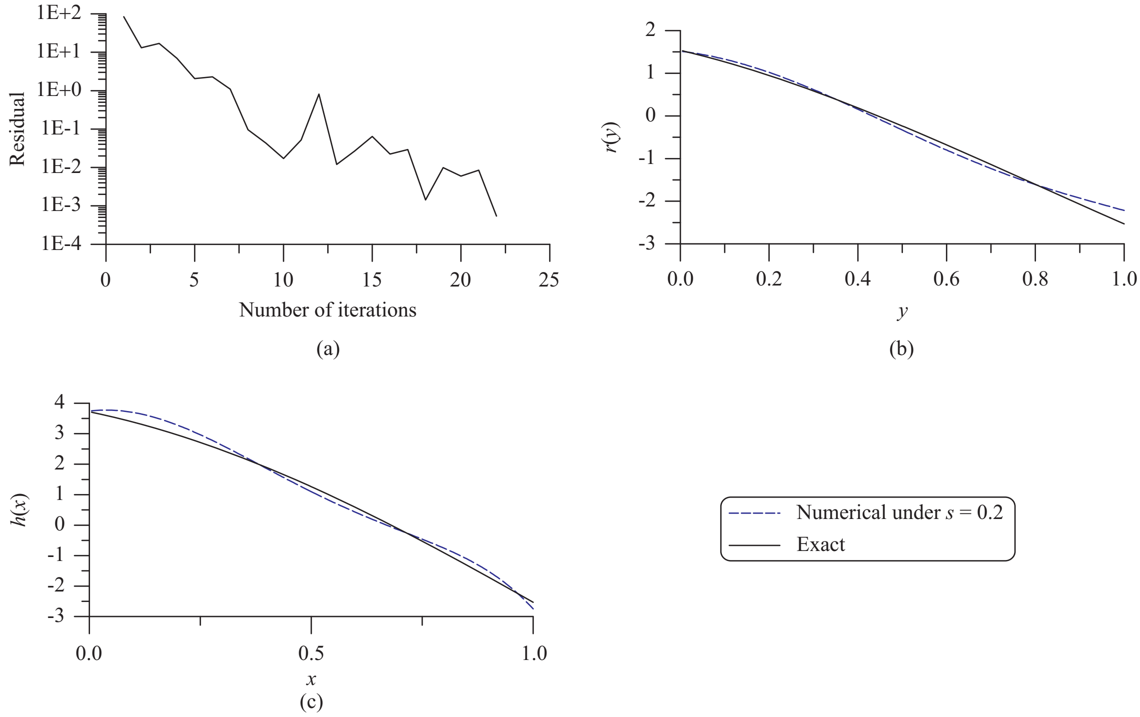

Fig. 7. For the second generalized inverse boundary value problem, (a) convergence rate, and comparing numerical and exact solutions of (b) $r(y)$, and (c) $h(x)$ for example 5.

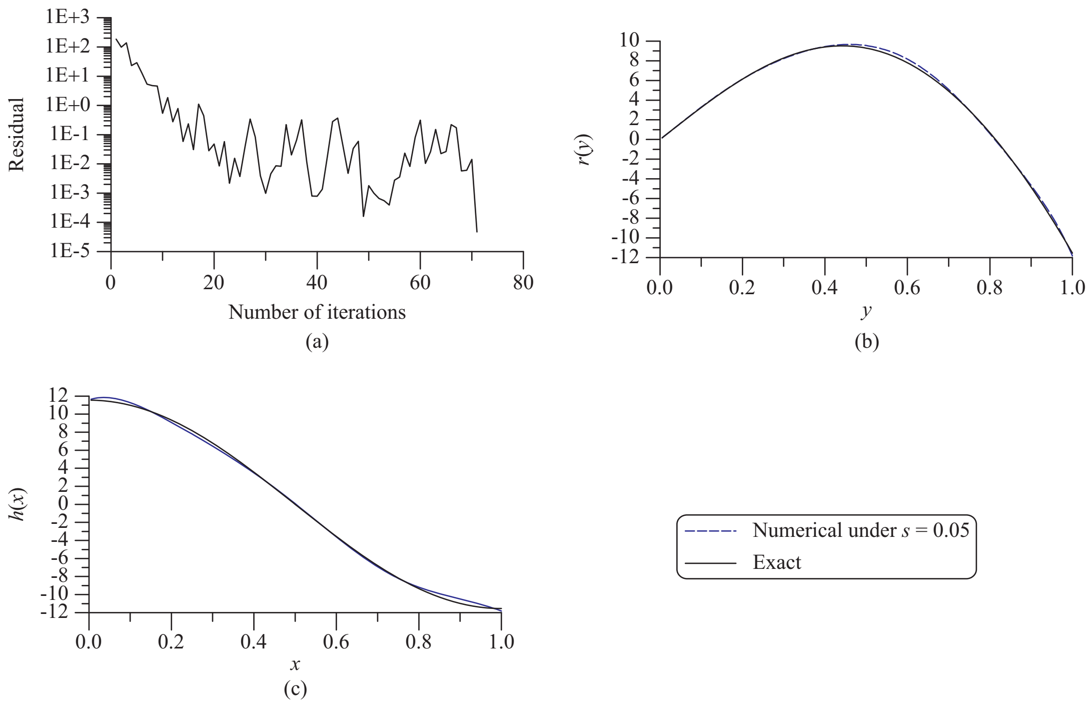

Fig. 8. For the second generalized inverse boundary value problem, (a) convergence rate, and comparing numerical and exact solutions of (b) $r(y)$, and (c) $h(x)$ for example 6.

a large noise $s = 0.2$, the BIEM is convergence with 22 steps as shown in Fig. 7(a), where the convergence criterion is given by $\varepsilon = 10^{-3}$. In Fig. 7(b), we compare the numerical recovery of $r(y)$ with the exact one, whose maximum error is 3.14×10^{-1}, while the numerical recovery of $h(x)$ with the exact one is shown in Fig. 7(c), whose maximum error is 3.47×10^{-1}. The recovered

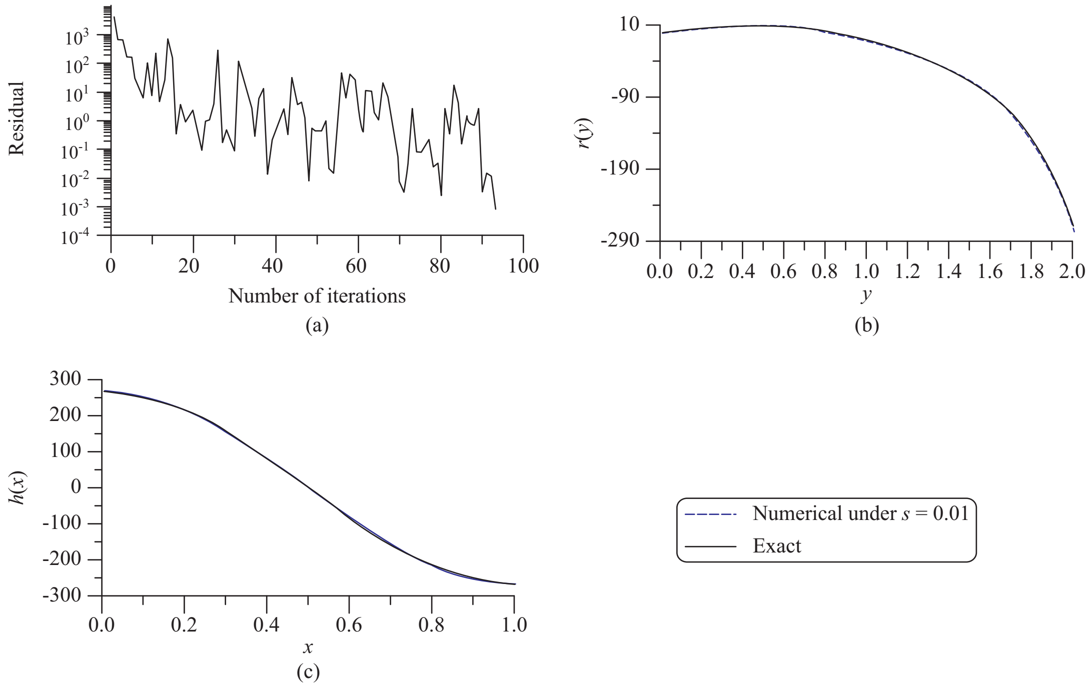

Fig. 9. For the second generalized inverse boundary value problem, (a) convergence rate, and comparing numerical and exact solutions of (b) $r(y)$, and (c) $h(x)$ for example 6.

results are close to the exact ones even a large noise is added.

2. Example 6

We consider a more difficult second problem with

$$u(x, y) = \cosh(\pi x)\sin(\pi y) + \cos(\pi x)\sinh(\pi y) . \quad (34)$$

in a unit square. We take $m_1 = m_2 = m_4 = m_5 = 10$, $m_3 = 3$ and $m_0 = 3$. The BIEM is convergence with 71 steps as shown in Fig. 8(a), where the convergence criterion is given by $\varepsilon = 10^{-4}$ and the noise is $s = 0.05$. In Fig. 8(b), we compare the numerical recovery of $r(y)$ with the exact one, whose maximum error is 3.68×10^{-1}, while the numerical recovery of $h(x)$ with the exact one is shown in Fig. 8(c), whose maximum error is 4.94×10^{-1}. The recovered results are close to the exact ones even when a large noise is added.

Finally, We take a larger domain with $a = 1$, $b = 2$. The BIEM is convergent with 93 steps as shown in Fig. 9(a), where the convergence criterion is given by $\varepsilon = 10^{-3}$ and the noise is $s = 0.01$. In Fig. 9(b) we compare the numerical recovery of $r(y)$ with the exact one, whose maximum error is 4.94×10^{-1}, while the numerical recovery of $h(x)$ with the exact one is shown in Fig. 9(c), whose maximum error is 8.4×10^{-1}.The recovered results are close to the exact ones.

VII. CONCLUSIONS

For the generalized inverse boundary value problems of Laplace equation in a rectangle, we proposed two new problems with three boundary functions and two boundary functions being specified, and we recovered other boundary functions on the portions where the data are missing. By using the technique of a boundary integral equation method together with a specially designed test function we have completed the boundary data by requiring some extra data. The test function is chosen such that it is zero on three boundaries; there exists no Trefftz test function which is zero on four boundaries. This test function rendered a simple integral equation to complete the boundary data. Then we can solve the Laplace equation under the given data and recovered data to find the numerical solution in the interior nodal points. Although the generalized inverse boundary value problems are more difficult than the Cauchy problem, we can solve them quite accurately and highly efficiently under large noise up to 10% and 20%.

REFERENCES

Brühl M. and M. Hanke (2000). Numerical implementation of two noniterative methods for locating inclusions by impedance tomography. Inverse Problems 16,1029-1042.

Chang, J. R., W. Yeih and M. H. Shieh (2001). On the modified Tikhonov's regularization method for the Cauchy problem of the Laplace equation. Journal of Marine Science and Technology 9, 113-121.

Chi, C. C., W. Yeih and C.-S. Liu (2009). A novel method for solving the Cauchy problem of Laplace equation using the fictitious time integration method. Computer Modeling in Engineering and Sciences 47, 167-190.

Cimetière, A., F. Delvare, M. Jaoua and F. Pons (2001). Solution of the Cauchy problem using iterated Tikhonov regularization. Inverse Problems 17, 553-570.

Essaouini, M., A. Nachaoui and S. E. Hajji (2004). Numerical method for solving a class of nonlinear elliptic inverse problems. Journal of Computational and Applied Mathematics 162, 165-181.

Fang, W. and M. Lu (2004). A fast collocation method for an inverse boundary value problem. International Journal for Numerical Methods in Engineering 21, 1563-1585.

Fu, C. L., X. T. Xiong and Z. Qian (2007). Fourier regularization for a backward heat equation. Journal of Mathematical Analysis and Applications 331, 472-480.

Fu, C. L., H. F. Li, Z. Qian and X. T. Xiong (2008). Fourier regularization for a backward heat equation. Inverse Problems in Science and Engineering 16, 159-169.

Jourhmane, M. and A. Nachaoui (1999). An alternating method for an inverse Cauchy problem. Numerical Algorithms 21, 247-260.

Jourhmane, M. and A. Nachaoui (2002). Convergence of an alternating method to solve the Cauchy problem for Poisson's equation. Journal of Applied Analysis 21, 1065-1083.

Jourhmane, M., D. Lesnic and N. S. Mera (2004). Relaxation procedures for an iterative algorithm for solving the Cauchy problem for the Laplace equation. Engineering Analysis with Boundary Elements 28, 655-665.

Knowles, I. (1998). A variational algorithm for electrical impedance tomography. Inverse Problems 14, 1513-1525.

Liu, C.-S. (2008a). A highly accurate MCTM for inverse Cauchy problems of Laplace equation in arbitrary plane domains. Engineering Analysis with Boundary Elements 32, 778-785.

Liu, C.-S. (2008b). A modified collocation Trefftz method for the inverse Cauchy problem of Laplace equation. Computer Modeling in Engineering and Sciences 35, 91-111.

Liu, C.-S. (2012). Optimally scaled vector regularization method to solve ill-posed linear problems. Applied Mathematics and Computation 218, 10602-10616.

Liu, C.-S. (2013). A two-side equilibration method to reduce the condition number of an ill-posed linear system.. Computer Modeling in Engineering and Sciences 91, 17-42.

Liu, C.-S. (2014). The pre/post equilibrated conditioning methods to solve Cauchy problems. Engineering Analysis with Boundary Elements 40, 62-70.

Liu, C.-S. (2016). A simple Trefftz method for solving the Cauchy problems of three-dimensional Helmholtz equation. Engineering Analysis with Boundary Elements 63, 105-113.

Liu, C.-S. (2017). A global domain/boundary integral equation method for the inverse wave source and backward wave problems. Inverse Problems in Science and Engineering 25, 506-531.

Liu, C.-S. and S. N. Atluri (2013). Numerical solution of the Laplacian Cauchy problem by using a better postconditioning collocation Trefftz method. Engineering Analysis with Boundary Elements 37, 74-83.

Liu, C.-S. and C. W. Chang (2012). A novel mixed group preserving scheme for the inverse Cauchy problem of elliptic equations in annular domains. Engineering Analysis with Boundary Elements 36, 211-219.

Liu, C.-S. and C. W. Chang (2016). A global boundary integral equation method for recovering space-time dependent heat source. International Journal of Heat and Mass Transfer 92, 1034-1040.

Liu, C.-S. and C. L. Kuo (2011). A spring-damping regularization and a novel Lie-group integration method for nonlinear inverse Cauchy problems. Computer Modeling in Engineering and Sciences 77, 57-80.

Liu, C.-S. C. L. Kuo and D. Liu (2011). The spring-damping regularization method and the Lie-group shooting method for inverse Cauchy problems. Computer, Materials & Continua 24, 105-123.

Liu, C.-S., W. Qu, W. Chen, and J. Lin (2017). A novel Trefftz method of the inverse Cauchy problemfor 3D modified Helmholtz equation. Inverse Problems in Science and Engineering 25, 1278-1298.

Nachaoui, A. (2004). Numerical linear algebra for reconstruction inverse problems. Journal of Computational and Applied Mathematics 162,147-164.

Yeih, W., T. Koya and T. Mura (1993). An inverse problem in elasticity with partially overspecified boundary conditions. Part I: theoretical approach. ASME Journal of Applied Mechanics 60, 595-600.